



Physical drivers and trends of the recent delayed withdrawal of the Southwest

2 **Monsoon over Mainland Indochina**

- 3 Kyaw Than Oo ^{1, 2, *}, Chen Haishan¹, Kazora Jonah^{1,3}, Du Xinguan¹
- 4 ¹ Key Laboratory of Meteorological Disaster, Ministry of Education/Joint International Research
- 5 Laboratory of Climate and Environment Change/Collaborative Innovation Center on Forecast and
- 6 Evaluation of Meteorological Disasters, Nanjing University of Information Science and Technology,
- 7 Nanjing, 210044, People's Republic of China
- 8 ² Aviation Weather Services, Yangon, Myanmar
- 9 ³ Rwanda Meteorology Agency, Kigali, Rwanda
- *Corresponding author: kyawthanoo34@outlook.com, https://orcid.org/0000-0003-1727-3462

11 Key point

18

- Cumulative Change of Mainland Indochina Southwest Monsoon (MSwM) new definition
 index improves understanding of monsoon transitions.
- Anomalous trends of Subtropical Westerly Jet and Tropical Easterly Jet are linked to changes
 in wind patterns and monsoon timing.
- Anomalous Sea surface temperatures impact moisture transport during MSwM Retreat
 phases.

Plain Language Summary

- 19 The study investigates the delay withdrawal of the Mainland Indochina Southwest Monsoon (MSwM)
- 20 by using spatial trend connections with meteorological and oceanic factors. The new Cumulative
- 21 Change-Point Monsoon (CPM) definition index well described the definition of monsoon seasonal
- 22 shifting. The results show that the subtropical westerly jet is getting stronger while the tropical easterly
- 23 jet is getting weaker within these years. This influences the regional wind patterns and delays the
- 24 monsoon withdrawal. The study highlights the critical role of ocean-atmosphere interactions and local
- 25 atmospheric circulation in influencing the summer monsoon. Specifically, warmer sea surface
- 26 temperatures in the Indian Ocean enhance moisture transport through strengthened southwesterly
- 27 winds, while atmospheric pressure gradients drive moisture convergence over the region. These
- 28 processes contribute to prolonged monsoon seasons, increasing the risk of floods and disrupting
- 29 agricultural schedules, which significantly impact water management and farming in Mainland
- 30 Indochina.





Abstract

31

45

46

32 The study investigates the key factors that cause the Mainland Indochina Southwest Monsoon (MSwM) 33 to delay withdrawal, utilizing a spatial trend correlation between the monsoon index and various 34 meteorological and oceanic variables such as sea surface temperature (SST), zonal winds, and moisture 35 transport. A significant strengthening trend in the Subtropical Westerly jet (SWJ) and a weakening 36 Tropical Easterly jet (TEJ) not only impacts regional wind patterns but also delays the monsoon 37 departure. The anomalous South China Sea and the equatorial Indo-Pacific Ocean surface temperature 38 (SSTA) further contribute to these delayed withdrawals, and there is a significant correlation between the MSwM withdrawal index and SSTA, moisture transport, and essential atmospheric factors. The 39 40 results clarify MSwM dynamics, offering significant insights for future climate research associated 41 with MSwM. The study also suggests that the variability of ocean-atmosphere interactions and local 42 atmospheric circulation patterns is critical for understanding monsoon variability, which has a potential 43 impact on climate predictions, water resource management, and agriculture practices over Mainland 44 Indochina.

Keywords: Mainland Indochina, Monsoon Withdrawal, MSwM, SWJ, TEJ, ENSO

1 Introduction

47 In tropical Asia, the summer monsoon system is one of the most significant meteorological 48 phenomena in the Northern Hemisphere. This monsoon onset and withdrawal are the most notable 49 intraseasonal variable in monsoon systems. The beginning of the summer rainy season, extensive 50 convection, and a rapid change in atmospheric circulation characterize this period (Aung et al., 2017; 51 Bordoni & Schneider, 2008; Salinger et al., 2014). Base on previous science literature of the Asia-52 Pacific monsoon classification, there are three primary types of summer monsoons, East Asian 53 (EASM), Indian (ISM), and Western North Pacific (WNPSM) monsoons (Wang & Ho, 54 2002), (Supplementary Fig S-1). The eastern bay of Bengal (EBOB), as known as the mainland-55 Indochina region (MIC) study area (Fig. 1a) is situated in a transitional zone between the (ISM and the WNPSM systems (Oo & Jonah, 2024). The monsoon indices had been developed to study the transition 56 57 and boundary between the Indian Summer Monsoon (ISM) and East Asian Summer Monsoon (EASM) 58 (Cao et al., 2012), characterize monsoon onset and withdrawal using rainfall-based metrics (Bombardi 59 et al., 2019; S. Zhang et al., 2024), and define these phases through circulation-based approaches (L. 60 Chen et al., 2023; Hu et al., 2022). The MIC also features complex terrain, with high mountain ranges 61 and long costal area. Simply, the MIC dominates a unique position between the southern areas of East 62 and Middle East Asia, where this monsoon system over MIC exhibiting transitional characteristics 63 between the two monsoon systems (Y. Zhang et al., 2002a). Consequently, significant variation in





- agricultural planting and ploughing times occur over MIC affected by the monsoon rainfall (Fig. 1b),
- depending upon the early or late monsoon onset or withdrawal.

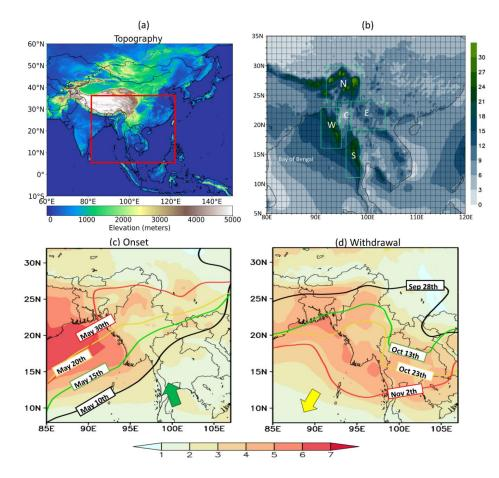


Fig. 1 (a) Topography (m) of the study area, including mainland Indochina. (b) Daily rainfall (mm) during the MSwM season. (c) Climatological onset and (d) withdrawal dates of MSwM with standard deviation values (shaded, days). This figure was created with Python 3.10 (Matplotlib 3.5.2 [https://matplotlib.org/], Cartopy 0.20.0 [https://pypi.org/project/Cartopy/]).

A range of onset and withdrawal indices has been established, based on rapid changes in extensive atmospheric structures. Especially, the most commonly used atmospheric variables for defining onset and withdrawal indices include rainfall (Ajayamohan et al., 2009; Colbert et al., 2015; Htway & Matsumoto, 2011; Vijaya Kumari et al., 2018), and reversable component wind (CY Li, 1999; Li et al., 2010; Webster & Yang, 1992). The summer monsoon typically onset to MIC between mid-May and early June, with slight variations in indices and statistics (Mao & Wu, 2007; Oo, 2023a; Ren et al., 2022; Wang & Ho, 2002). The MSwM withdrawal displayed significant interannual variability, with a extent of one to two weeks may vary among the earliest and latest withdrawals based on climatological data (Evan & Camargo, 2011; Oo, 2023a).





79 The global wind circulation and the El Niño Southern Oscillation (ENSO) have been widely 80 studied for their influence on the interannual variability of monsoon onset (Roxy et al., 2014; R. Wu, 81 2017), the formation of South Asia's subtropical high (Q Guo, 1988; Wang et al., 2008; Y. Zhang et 82 al., 2002b), and fluctuations in local sea surface temperature (SST) (Salinger et al., 2014; Xu et al., 83 2023). Based on these long-term physical atmospheric variables data, this study seeks to examine the 84 factors contributing to the delay withdrawal of the MSwM, with superior weight on ocean-atmosphere 85 interactions and zonal wind dynamics, which have been insufficiently explored in this area, since 86 monsoon rains are crucial for agriculture and fill up water supplies (Win Zin & Rutten, 2017; Zin Mie 87 Mie Sein et al., 2015). In this study, we present the variability of withdrawal dates over interannual 88 scale. Due to the significant up trending of local withdrawal date of MSwM, derived from the 89 combination of reversal of winds circulation (Ramage, 1971) and vertical moisture flux transport 90 changes (Fasullo & Webster, 2003). We investigate the mechanism driver of these delay withdrawal and potential driver of continues untimely rainfall after MSwM withdrawal. 91

92 **Data and Method**

- 93 The study utilizes data from five sources:
- 94 1. **Department of Meteorology and Hydrology, Myanmar (DMH)**: Daily observed rainfall, sea
- 95 level pressure, and annual onset and withdrawal dates for significant regions were collected from
- 96 DMH, which operates 79 meteorological stations nationwide. This data help assess validate of
- 97 reanalysis datasets.
- 98 2. NCEP/NCAR Reanalysis: This dataset provides zonal (u) and meridional (v) wind components,
- specific humidity (q), geopotential height (z), and vertical velocity (w) at atmospheric isobaric
- levels in the troposphere for wind analysis (Kanamitsu et al., 2002).
- 101 3. European Centre for Medium-Range Weather Forecasts ECMWF: ERA5 offers reanalysis
- data with a 0.25° geographical resolution for global climate analysis, including sea level pressure
- 103 (SLP), moisture flux convergence (MFC), and outgoing longwave radiation (OLR) for the period
- 104 from 1991 to 2020 (Hersbach et al., 2020).
- 4. Unified Gauge-Based Analysis of Global Daily Precipitation (CPC): This dataset provides
- rainfall data (M. Chen et al., 2008; Jiao et al., 2021).
- 5. *Hadley Centre*: Hadley Centre Sea Surface Temperature dataset (HadISST) (Selman & Misra,
- 108 2014).

109

2.1.1 Definition of Monsoon onset and withdrawal by CPM index

- 110 The MSwM region is defined by coordinates 10°N-30°N and 85°E-110°E (Fig. 1; see Appendix
- 111 for additional details). We examine seasonal fluctuations in the moisture budget and extensive
- atmospheric circulation, as established by:





113 Equation 1

114
$$\mathbf{MFC} = -\int_{Surface}^{300hPa} \nabla_{p} \cdot (\mathbf{U}q) \frac{dp}{g} = P - E + \frac{\partial W}{\partial t}$$

This equation was developed from a prior study on the variability of the Asian Monsoon (Walker et al., 2015). In this context, Moisture Flux Convergence (MFC) is a vital quantity that delineates the equilibrium of moisture in the atmosphere. The initial segment of the equation encapsulates the dynamic component, represented by the divergence of moisture flow "(Uq). ∇ p" denotes the movement and accumulation of moisture resulting from wind patterns. This dynamic element is essential for comprehending how atmospheric circulation patterns affect moisture availability. The second component, "P - E + ∂ W/ ∂ t" signifies the thermodynamic equilibrium of moisture inside the system. P represents precipitation, E signifies evaporation, and ∂ W/ ∂ t reflects temporal variations in water storage. This relationship illustrates how thermodynamic mechanisms regulate the moisture budget and influence the overall climate dynamics of the monsoon zone.

By integrating dynamic and thermodynamic aspects, the cumulative change of the MSwM (CPM) index provides a strong framework for analyzing the behavior of the monsoon circulation over time. Building upon the MFC, we define the Cumulative Change of the MSwM (CPM) index of onset as follows:

129 Equation 2

$$MSwM (CPM) = \frac{1}{5} * (D(U_1 - U_2) + D(P_1 - P_2) + D(MFC) + D(TP_{net}) + D(OLR))$$

We determine the normalized values for each factor annually for statistical investigation. The cumulative value change from positive to negative, or vice versa, is verified for further statistical calculations. "D" in Equation (2) expresses the date when the state shifts of positive or negative (+ to - or - to +) values and typically represents the change or difference in the standardize values of each variable in a year.

In this equation, D (U1- U2) and D(P1 - P2) represent the differences in zonal winds and pressure between the southern and northern regions of the Mainland Indochina (MIC). Specifically, the southern region (90°–100°E, 10°–15°N) reflects the influence of the broad Indochina Peninsula, where the southwest monsoon winds are most active, while the northern region (95°–100°E, 25°–30°N) captures the terrain-influenced pressure dynamics near the eastern Tibetan Plateau (Fig. 1a) and the southwest monsoon wind withdrawal pattern (Fig. 1d), we take pressure readings that are different from longitude ranges as two distinct regions. The meridional shear in the 850-hPa zonal winds and the pressure gradient between northern and southern regions which is driving monsoon flows, the key indicators of monsoon circulation, are averaged across two distinct regions: the southern MIC (90E-100E, 10N-

https://doi.org/10.5194/egusphere-2025-1159 Preprint. Discussion started: 16 April 2025 © Author(s) 2025. CC BY 4.0 License.



145

146

147

148

149

150

151

152

153

154

155156

157

158

159

160

161

162

163

164

165

166

167

168

169

170

171

172

173174

175

176

177



15N), referred to as (U1,P1), and the northern MIC (95E-100E, 25N-30N), designated as (U2,P2). The term D(MFC) captures the cumulative changes in moisture transport and convergence, essential for monsoon rainfall, while D(TPnet) represents net precipitation changes, indicating monsoon withdrawal as well as onset by rainfall and D(OLR) the changes in outgoing longwave radiation, closely linked to convective activity and cloud cover to confirm monsoon rainfall, respectively. We calculate the mean change date of the standardized positive/negative value of the outgoing longwave radiation (OLR), the vertically integrated moisture budget transition (MFC), the net precipitation (TpNet), the meridional shear wind (U1-U2) (U-wind), and the pressure differential (P1-P2) (dP). The first day of three consecutive positive or negative days is taken into consideration when determining the change date. Next, we obtained each variable's change point dates for every year. Lastly, the climatology data for every term date was acquired (Supplementary Table S1). We used these findings to compute the MSwM Change Point Index, which is the arithmetic mean onset dates, withdrawal dates, and season length (Supplementary Table S4). A student's t-test is used to calculate the correlation coefficients of these findings at the 95% level of significance. This rounded approach allows for a comprehensive assessment of the interrelationships among these parameters, simplifying the identification of key onset (Fig. 1c) and withdrawal (Fig. 1d). Moreover, common statistical methods such as correlation (Krugman et al., 2018), regression (Ma, 2019), random forest (Breiman, 2001), box and whisker (Schmidhammer, 2000) are also applied in the study at necessary parts.

The Random Forest technique, a widely used ensemble machine-learning method, was utilized to find the relative relevance of variables controlling monsoon withdrawal and rainfall. It generates several decision trees during training by sampling subsets of data and features, hence mitigating overfitting and enhancing generalization (Breiman, 2001). Our study incorporated input variables comprising atmospheric and hydrological factors, including Outgoing Longwave Radiation (OLR), Net Precipitation (Net), Moisture Flux Convergence (MFC), Zonal Wind Shear (U), and Pressure Differential (dP). Each tree generated a prediction, and the final output was ascertained by averaging (for regression tasks) or by majority voting (for classification tasks). Box and whisker plots were employed to graphically encapsulate the distributions of essential variables across various phases of the monsoon season (Schmidhammer, 2000). It is good to examine the day-of-year distributions for monsoon withdrawal timing based on many factors, including dP, U, MFC, Net Precipitation, and OLR. This analysis clearly exhibited variability and key tendencies in the data, highlighting the contribution of specific variables to withdrawal patterns. For example, zonal wind shear (U) exhibits narrower variability, indicating a more consistent relationship with withdrawal timing compared to other factors.





178 3 Results and Discussion

179 3.1 Climatology Outlook

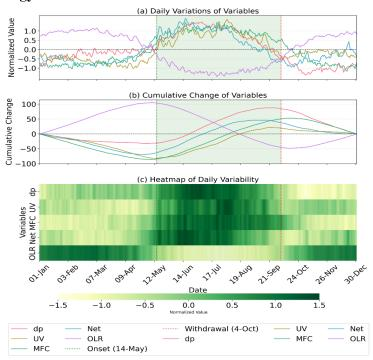


Fig. 2 Daily and cumulative variations of monsoon parameters with their seasonal progression. (a) Daily variations of normalized parameters: pressure gradient (dP; red), wind shear (UV; yellow), moisture flux convergence (MFC; green), net precipitation (Net; blue), and outgoing longwave radiation (OLR; purple). (b) Cumulative changes of the same parameters with identical color coding. (c) Color strip timeseires showing the daily variability of all parameters throughout the year. Vertical dotted lines indicate monsoon onset (green; 14-May) and withdrawal (red; 4-Oct), with light green shading highlighting the monsoon active period in (Fig a nd b). All parameters are normalized and calculated according to Eqs. (1) and (2). This figure was created using Python 3.10 with Matplotlib 3.5.2 (https://matplotlib.org/) and Sephorn

Fig. 2 explained how the MSwM (CPM) index is constructed by combining both thermodynamic and dynamic climatology daily contribution (Fig. 2.a) and their cumulative change (Fig. 2.b) of same variables. Cumulative change curves (CMFC, Cdp, Cwind) help track the transitions in atmospheric conditions that define the onset and withdrawal of the monsoon. The simultaneous positive and negative shifts in MFC, OLR, pressure differentials, and wind shear facilitate the identification and calculation of monsoon onset and withdrawal. Both figures underscore the significance of cumulative effects in the MSwM index, where prolonged alterations over several days in moisture flux, wind shear, and pressure differentials signify critical transitions in the monsoon cycle, thereby illustrating the seasonal progression of the monsoon in contrast to mere daily variations. The Color strip timeseries (Fig. 2.c) support more clarity transaction of monsoon season by same variables values. The climatology dates for each year are shown in Table S-1 and S-2 of the supplemental material.





The India Monsoon Index (IMI), the Webster and Yang monsoon index for Asia (WYI), the West North Pacific monsoon index (WNPMI), and are some of the well-known monsoon indicators for the South Asian region (Goswami et al., 1999; Wang et al., 2001, 2004; Webster & Yang, 1992). However, seasonal wind variation and uniform rainfall can also be used to designate MSwM zones as sub-regions (Oo, 2022a, 2023b). In terms of annual variability, MSwM and other South Asian monsoon indicators show a comparable time-series pattern and a positive moderate connection (Supplementary Fig S-6).

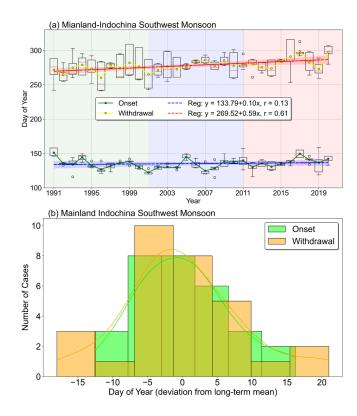


Fig. 3 (a) Interannual variability of MSwM onset (green line) and withdrawal (yellow line) dates, with trends. (b) Frequency distribution of deviations from mean onset and withdrawal dates, with implications for Indochina agriculture. This figure was created with Python 3.10 (Matplotlib 3.5.2 [https://matplotlib.org/]).

Examining the distribution patterns of the onset and withdrawal dates of the MSwM across MIC is interesting, despite the MSwM index reflecting changes in the whole MIC rather than a specific region within its domain. In this study, we only consider interannual variability over southern region (95E-100E, 10N-15N) ("S" area in Fig. 1.b) where is the first onset point (during onset) and last withdrawal point (during withdrawal) in north-south-north shifting of monsoon characteristic due to its role in the migration of the Intertropical Convergence Zone (ITCZ), which shifts northward during

https://doi.org/10.5194/egusphere-2025-1159 Preprint. Discussion started: 16 April 2025 © Author(s) 2025. CC BY 4.0 License.



216217

218

219

220

221

222

223

224

225

226

227

228

229

230

231

232

233

234

235

236

237



boreal summer, initiating intense convective activity and precipitation. At this latitude, the strong landocean thermal contrast generates a pressure gradient, drawing moist southwesterly winds from the Indian Ocean that converge and bring rainfall (Goswami & Xavier, 2005). This region aligns with the early onset of monsoon rainbands and moisture convergence observed in climatological data, as well as the geographical position of southern Myanmar, India and Sri Lanka, which are the first landmasses to experience the advancing monsoon (K Lau, 2000). Fig. 3.a shows interannual variation of onset and withdrawal dates with their trend including whisker statistical box. It indicates the timing of onset and withdrawal phases, which are vital for understanding how the regional monsoon system is developing. Over the MIC, early or delayed onset and withdrawal of the monsoon can dramatically affect the seasonal rainfall patterns, which may lead to regional crop production and society plans. The trend lines in both phases suggest possible long-term shifts in monsoon behavior (Fig. 3.a), may be influence of the broader climatic drivers such as variability of ENSO or Indian Ocean dipole (IOD) (Ding et al., 2011a; Wang & Ho, 2002). The timeseries trend displayed that withdrawal dates are significantly greater variation than onset dates within five variables of CPM index for each year especially in dynamic boundary (Fig. 4). The frequency distribution of deviations from the mean onset and withdrawal dates (Fig. 3.b), which explained that onset and withdrawal date may early or delay generally one to two weeks (5 to 7 days as usual in general). The longest delay (early) withdrawal phases occurred with 20 days (15 days) during this 30-year study period 1991-2020. The onset phases are generally characterized by a rapid shift in moisture flux and dynamic transformations over MIC, whereas the withdrawal phases occurs more gradually and may be affected by extensive atmospheric patterns (Seager et al., 2010), including modifications in subtropical jets, mid-latitude disturbances, and tropical easterly waves, which can introduce variability in the timing of the retreat (Hu et al., 2019).



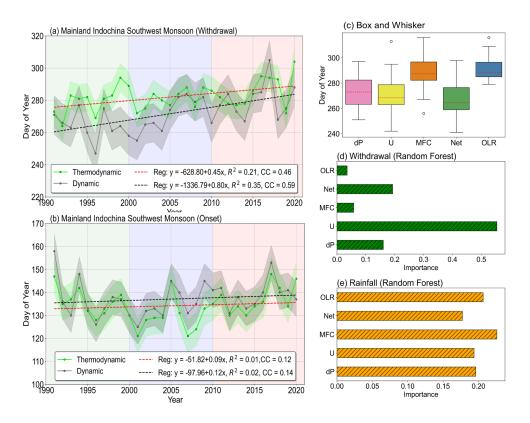


Fig. 4 Interannual variation of thermodynamic and dynamic factors during (a) onset and (b) withdrawal phases of MSwM, with trends, highlighting the impact on mainland Indochina. (c) the box whisker plot of five physical parameters to determine the MSwM onset and withdrawal (Oo etl. 2023). And their sensitivity tests by random forest method (d) for CPM index and (e) for monsoon regional rainfall. This figure was created with Python 3.10 (Matplotlib 3.5.2 [https://matplotlib.org/]).

The interannual variation trends of the onset and withdrawal dates of MSwM from 1991 to 2020, have a clear divergence in behavior between the two phases while studied split into dynamic and thermodynamic according to CPM index (Fig. 4). The onset of the MSwM shows slight changes over time, with weak regression slopes of 0.09 and 0.12 days per year for the thermodynamic and dynamic components respectively under weak statistically significant (Fig. 4.b). However, the withdrawal phase exhibitions a much more marked positive trend, especially the dynamic component has an even steeper slope of 0.80 days per year, while thermodynamic component for withdrawal shows a regression slope of 0.45 days per year with 95% statistically significant respectively (Fig. 4.a). This indicates that dynamic factors, such as changes in large-scale wind patterns, are playing a more significant role in driving the delayed monsoon withdrawal.

The box plot (Fig. 4.c) reveals that MFC and OLR correspond to delay withdrawal dates, indicating that delayed MFC may play key roles in postponing the withdrawal. The result is generally correct due to the rainfall days remaining due to regional local convective activities and tropical



258

259

260

261

262

263

264

265

266

267

268

269

270

271

272

273

274

275

276

277

278

279

280

281

282

283

284

285286

287



cyclone effect during the post monsoon season (Akter & Tsuboki, 2014; Fosu & Wang, 2015; Oo et al., 2024). When we go dive into this, Fig. 4.e displays that monsoon rainfall variability is impacted by U, dP, MFC, and OLR, though their standing is more evenly spread, the random forest results highlight U (850-hPa zonal wind) as the most critical factor driving the withdrawal, followed by dP (Fig. 4.d). The strong influence of U suggests that zonal wind shifts, possibly linked to tropical disturbances such easterly wave from south China sea, upper jest stream anomaly, local tropical cyclones, could further affect the timing of withdrawal. This indicates that rainfall events are still remain usual even after the monsoon winds was withdrawal from the study region (Chou et al., 2009). To reach this conclusion, we will go further into the next section.

3.2 Variation of MSwM withdrawal dates and Rainfall in October

The first Empirical Orthogonal Function (EOF) modes of October rainfall and mean sea level pressure over the study area, and their normalized principal components (PCs) expressed in Fig. 5. The first EOF for rainfall, explaining 34.4% of the variance (Fig. 5.a) and the first EOF for MSLP, explaining a larger 81.5% of variance, indicating its stronger influence on regional climate (Fig. 5.b). Positive and negative eigenvectors suggest the impact of MSLP and rainfall distribution over withdrawal phases that reduction in rainfall and increasing in pressure. The regression between monsoon withdrawal dates by MSwM definition index (CPM) and regional rainfall explained positive relations (green areas in Fig. 5.c) suggest that the index can significantly reflect the October rainfall over the study area with 95% confidence. This show CPM index is significantly reflected to southern MIC ("S" area in Fig. 1.b), where is the last point of monsoon withdrawal, regional rainfall during withdrawal phases. Moreover, PCs time series of rainfall (RF), and SLP, from 1991 to 2020 (Fig. 5.d), are comparing with monsoon withdrawal dates and the correlation between withdrawal dates and SLP shows 0.41, and between RF exhibited 0.24, with statistically confidence (p > 0.05). However, the weak correlation between withdrawal timing and PCs RF suggests that while the timing of monsoon withdrawal affects the overall seasonal rainfall, it does not directly influence the spatial distribution of rainfall. This is because spatial distribution is primarily governed by local factors such as topography, moisture transport, and mesoscale atmospheric dynamics rather than the withdrawal timing alone. A late withdrawal may extend the period of rainfall over certain regions, increasing total rainfall. This dominant EOF modes capture the large-scale spatial variability of October rainfall and sea level pressure pattern, which is vital for understanding the dynamics of the transition from the warm wet southwest monsoon to the cold dry northeast monsoon season over MIC (Hannachi, 2004; Oo, 2022b; X. Wu & Mao, 2018).



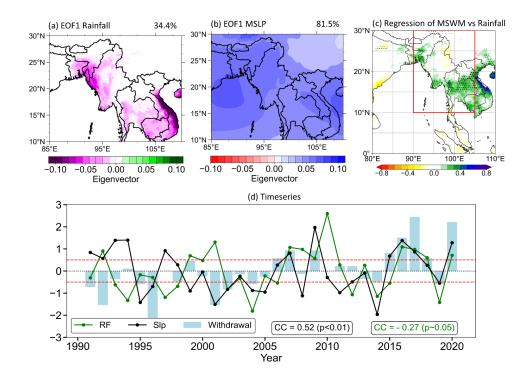


Fig. 5 First EOF modes of (a) rainfall and (b) Slp. (c) The regression values of withdrawal CPM indexd and regional october rainfall with dotted area of 95% statistically confident by t-test. (d) The interannual variation of normalized PCs of first two EOF and normalized MSwM withdrawal dates with their correlation CC by respective color. The horizontal red dotted sperated the late (>0.5) and early (< -0.5) witdrawal years by their normalized anoamlies varues. This figure was created with Python 3.10 (Matplotlib 3.5.2 [https://matplotlib.org/], Cartopy 0.20.0 [https://pypi.org/project/Cartopy/]).

In addition, the SLP patterns are directly related to the atmospheric circulation that initiatives rainfall and weather conditions over the region (Loikith et al., 2019). The shift in the SLP pattern could indicate changes in the positioning of the low-level monsoon winds and subtropical high-pressure systems, which bring the moisture-flux into mainland Indochina (Liu et al., 2021) (Fig S-5 in supplementary). The PCs associated with these modes provide a temporal perspective, indicating how these dominant patterns advance over time. To perform composite analysis we collected eight delay withdrawal years (2006, 2007, 2009, 2015, 2016, 2017, 2018 and 2020) and eight early withdrawal years (1991, 1992, 1995, 1996, 2001, 2002, 2004 and 2019) by anomalies timeseries with PCs, we collected positive(negative) 0.5 (+/- renormalize 5-7 days) values years into late (early) withdrawal years.

3.3 Composite

The composite anomalies analysis of three majors' variables what are used to define monsoon onset and withdrawal are explained in Fig. 6. The climatological values between early years (first column) and late years (middle column), with their percentage difference (last column) over mainland



Indochina, were compared. The analysis indicates notable patterns in the distribution of monsoonal rainfall, especially in southern MIC. The difference % map delineates areas where rainfall has either diminished or increased, namely over southern MIC (Fig. 6.a and b). Their different percentages also result significantly in the same region as shown in Fig. 6.c. This confirmed that the most accurate classification skill of the MSwM CPM index over this southern MIC region as in (Fig. 5.c).

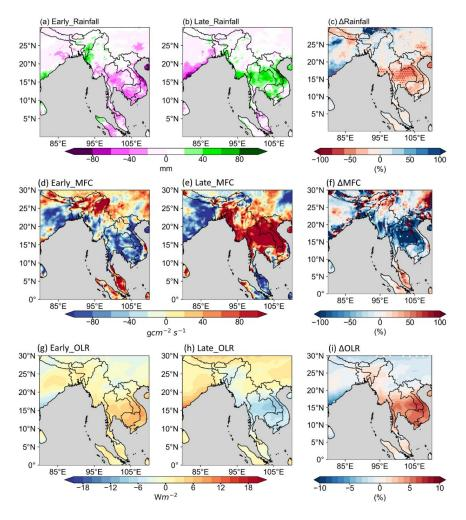


Fig. 6 Climatological anomalies mean rainfall (mm), MFC (g/cm²/s) and mean OLR (Wm²) for (a,d,g) early years, (b,e,h) late years, and (c,f,i) the percentage difference, illustrating changing moisture dynamics over mainland Indochina. Red dotted show the area of 95% statistically confident by t-test. This figure was created with Python 3.10 (Matplotlib 3.5.2 [https://matplotlib.org/], Cartopy 0.20.0 [https://pypi.org/project/Cartopy/]).

Changes in Moisture Flux Convergence (MFC) also impact rainfall patterns, with decreased MFC potentially reduction rainfall and increasing it, leading to wet conditions (Fig. 6.c and d). The figure compares climatologically to mean MFC in low-lying areas over southern MIC show similar negative/positive patterns is validation by their different values (Fig. 6.f). Same patterns are also found



328

329

330

331



for OLR of early and late withdrawal years over southern MIC. Thus, the MSwM CPM index is significantly reflected in this area.

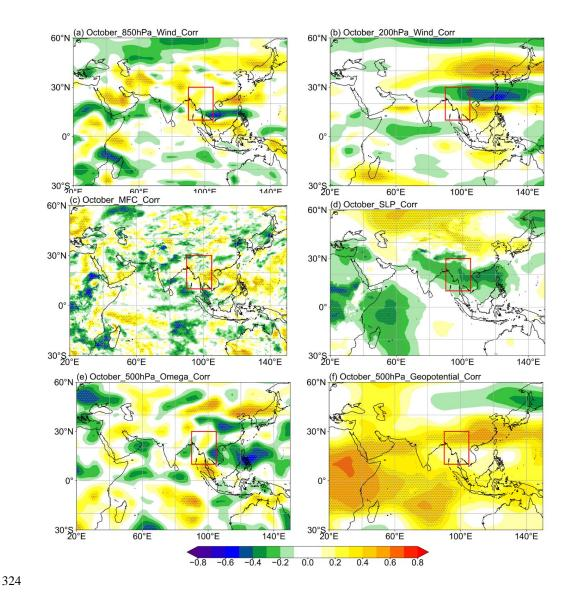


Fig. 7 Correlation between withdrawal date and October (a) 850 hPa wind, (b) 200 hPa wind, (c) MFC, (d) SLP, (e) 500 hPa Omega, and (f) 500 hPa geopotential, highlighting the drivers of monsoon withdrawal in mainland Indochina. Dotted shows the area of 90% statistically confident by t-test. This figure was created with Python 3.10 (Matplotlib 3.5.2 [https://matplotlib.org/], Cartopy 0.20.0 [https://pypi.org/project/Cartopy/]).

The correlation between these various atmospheric variables, showing how relation of these variables with the delayed monsoon withdrawal (Fig. 7). The correlation between the withdrawal date and wind speed was calculated at each grid point, analyzing the withdrawal date against both the u-





component and v-component speed. Statistical significance was determined using a student's t-test, with the dotted areas marking regions where the correlation is significant at the 90% confidence level. The correlations for 850 hPa wind speed (Fig. 7.a) expose strong negative relationships over MIC, indicating that weaker low-level winds contribute to the delay in withdrawal. This aligns with the positive-negative-positive trend pattern as in the Fig. 8.a and c, where negative correlations suggest a weakened low-level wind over MIC. In contrast, the 200 hPa wind correlation (Fig. 7.b) shows a positive relationship, particularly over the northern regions, suggesting stronger upper-level winds during delayed monsoon retreat periods, which likely strengthens the subtropical westerly jet (SWJ) region and weakening in Tropical Easterly Jet region (TEJ). The SWJ, defined as a dominant westerly wind stream at approximately 200 hPa in mid-latitudes, and the TEJ, a tropical Easterly wind at similar altitudes. Similar patterns are also exhibited in trend plots Fig. 8. b and d. A delayed withdrawal sustains the thermal gradient between the Indian Ocean and the Asian continent, maintaining a strong meridional temperature gradient in the upper troposphere and thereby intensifying the SWJ. Simultaneously, the TEJ weakens due to reduced upper-tropospheric divergence and the diminishing impact of tropical heating as the monsoon season transitions.

The correlation with Moisture Flux Convergence (MFC) (Fig. 7.c) also specifies a significant positive relationship in key study areas and positive trends also exhibited over same area (Fig S-7 in supplementary). This positive trend suggests that delayed monsoon withdrawal is associated with stronger moisture convergence, trapping moisture likely to experience rainfall in southern MIC for a longer period and it's also association with previous composite analysis as in Fig. 6. The Sea Level Pressure (SLP) correlation (Fig. 7.d) also shows a study area of negative correlation, which suggests that lower pressure systems dominate during delayed withdrawal, promoting cyclonic activities that extend the monsoon season and rainfall. Meanwhile, the positive correlations with 500 hPa Omega (Fig. 7.e) highlight the role of vertical motion over southern MIC, where positive Omega values (upward motion) correlate with a delayed withdrawal, can lead to cloud formation and rainfall if the conditions are right. Moreover, the 500 hPa geopotential positive correlations (Fig. 7.f) also show a weakened mid-tropospheric ridge over the subtropics with positive trend (Fig S-7 in supplementary), leading to the late monsoon withdrawal as the atmospheric circulation shifts.

The wind trends and anomalies highlight a significant alteration in both the lower (850 hPa) and upper (200 hPa) wind patterns (Fig. 8). The 850 hPa wind pattern (Fig. 8.a) indicates a weakening easterly flow over the South China Sea and southern MIC, and the 200 hPa wind trend (Fig. 8.b) indicates an intensification of the westerly flow linked to the SWJ, enhancing the upward motion and which may lead to anomaly lower-upper dynamic circulation patterns, and it may lead to delaying the timing of seasonal withdrawal of the monsoon. There is a noticeable positive-negative zonal wind





anomaly pattern, especially at the 200 hPa level, in the difference in wind structure between late and early years (late years minus early years) at both altitudes, and this pattern changes significantly over time (Fig. 8.c and d). Delays in the MSwM withdrawals are directly affected by changes in jet stream dynamics, such as the strengthening of the SWJ and the weakening of the Tropical Easterly Jet (TEJ). The results of these additional investigations provided confirmation of this pattern of dynamic abnormality. Specifically, across the SWJ and TEJ regions, variations in wind intensity and direction are critical in affecting the delayed withdrawal trend, according to the CPM index analysis of these dynamic circulation patterns. Important regions where wind anomalies are strongly linked to delayed withdrawal are highlighted by the plus and minus signs in the Fig. 8. This emphasizes as they indicate critical areas where wind anomalies are closely associated with delayed withdrawal.

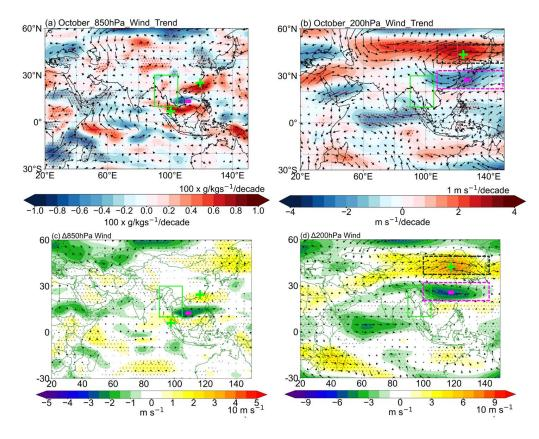


Fig. 8 The spatial trend of (a) 850hPa horizontal moisture transport(g/kgs⁻¹) and 200hPa wind component (m/s). Percentage difference (late minus early) in horizontal wind patterns at (c) 850 hPa, and (d) 200 hPa between late and early years of MSwM withdrawal month October during 1991-2020. Red and grey dotted show the area of 95% statistically confident by t-test. This figure was created with Python 3.10 (Matplotlib 3.5.2 [https://matplotlib.org/], Cartopy 0.20.0 [https://pypi.org/project/Cartopy/]).

The vertical structure of zonal wind, vertical motion, and moisture transport, comparing early and late years of the monsoon are exhibited in Fig. 9. The cross-section of vertical velocity over mainland Indochina, which is essential for understanding how wind circulation at different

https://doi.org/10.5194/egusphere-2025-1159 Preprint. Discussion started: 16 April 2025 © Author(s) 2025. CC BY 4.0 License.





atmospheric layers contributes to vertical motion and convective processes (Kotal et al., 2014; Sawyer, 1947). The weak upward motion over MIC had occurred during the early years (Fig. 9.a) and found exceeds and shifts northward during the late years as a reverse (Fig. 9.b). This reflects a strengthening in monsoon intensity and this is consistent with the observed weakening of TEJ, which decreases upper-level divergence and leads to delayed monsoon withdrawal.

The strong walker circulation over the study regions in the early years (Fig. 9.c), and weakens in the late years (Fig. 9.d) are suggests that the significant of TEJ and vertical circulation have declined, contributing to the delayed monsoon withdrawal. The reduced convective activity and moisture transport highlights how weaker jets are affecting monsoon dynamics (Roxy et al., 2015).



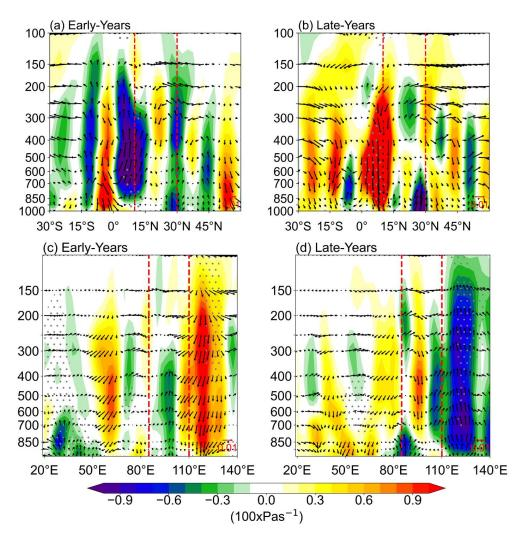


Fig. 9 Vertical cross section of omega (Pas⁻¹) of longitudinal averaging over (90°E-110°E) and latitudinal averaging (10°N-30°N) (a,c) for early years, (b,d) for late years. Grey dotted show the area of 95% statistically confident by t-test. This figure was created with Python 3.10 (Matplotlib 3.5.2 [https://matplotlib.org/], Cartopy 0.20.0 [https://pypi.org/project/Cartopy/]).

The analysis of the correlation (Fig. 7) and trend (Fig. 8) exhibited feature the critical role of atmospheric circulation patterns in influencing the delayed MSwM withdrawal. Extended moisture convergence and delayed withdrawal of monsoon systems are caused by the SWJ's strengthening and the TEJ's weakening at 200 hPa. Previous research has shown that conditions are conducive for extended monsoon motion when lower-level easterlies weaken, and upper-level westerlies intensify. This conclusion lends credence to those earlier findings (Krishnamurti et al., 2012; Roxy et al., 2015). In addition, prior research has demonstrated the connection between sustained moisture transport and extended convective activity with the monsoon, which is supported by the positive link between moisture flux convergence and delayed monsoon withdrawal (Goswami et al., 2006). The atmospheric





dynamics anomaly, specifically the weakening of the TEJ and the intensification of the SWJ, are significant variables influencing the noted trend of delayed monsoon withdrawal.

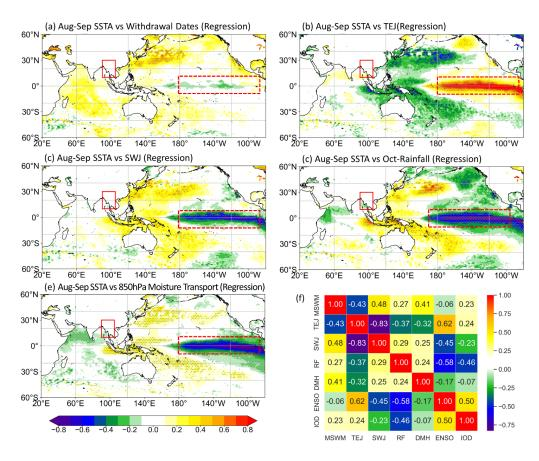


Fig. 10 Regression between Aug-Sep Sea surface temperatures (SSTs) and (a) MSwM withdrawal dates, (b) October tropical easterly jet, (c) October sub-tropical westerly jet, (d) October rainfall over MIC and (e) October 850hPa moisture divergent. Dotted hatches mean 95% confident area by t-test statically. The red boxed show MSwM region and red dotted box show the area in the Pacific with the strongest negative positive correlation. (f) Correlation heatmap between variables used in this study. DMH refers to the MSwM withdrawal dates from National weather services recorded. This figure was created with Python 3.10 (Matplotlib 3.5.2 [https://matplotlib.org/], Cartopy 0.20.0 [https://pyth.org/project/Cartopy/]).

The relationship between August-September SST anomalies and the delayed withdrawal of the MSwM showing not significant correlation over the equatorial Pacific Ocean (Fig S-9, supplementary), indicating that negative anomaly SSTs in this region are associated with delayed monsoon withdrawal (Fig. 10.a). This is constant with the role of warm SSTs over Indochina region are maintaining convective activity (Roxy et al., 2015; Krishnan et al., 2016) and preventing the on-time withdrawal of the monsoon however cold SSTs over Niño3-4 region does not directly impact on withdrawal dates. The red dotted boxed region shows the area in the Pacific with the strongest negative/positive correlation, suggesting a link between SST anomalies in the central Pacific and the timing of monsoon withdrawal. The relationship between SST and the tropical easterly jet (TEJ) and subtropical westerly





jet (SWJ) in October, the strong positive correlation between SST and TEJ over the Pacific Ocean (Fig S-9.b, supplementary) suggests that warmer SSTs exceeding the strength of TEJ (Fig. 10.b). This agreed with the previous trend and composite finding (Fig. 8) that the weakening of the TEJ is a critical factor in delaying the monsoon withdrawal. The weakening of the TEJ boost the lower-level monsoon circulation to endure for an extended duration over MIC (Huang et al., 2020; Sreekala et al., 2014). In contrast, Fig. 10.c shows a negative regression between SST and SWJ, this demonstrates that cooler SSTs over same area also strengthen the SWJ. This finding supports the idea that a positive anomalies SWJ also impact to delayed withdrawal (Dimri et al., 2015; Sreekala et al., 2014).

The Aug-Sep SST of tropical Pacific and Indian ocean and rainfall within October can also predict to MIC October rainfall. The negative correlation otherwise (La Niña) in the equatorial Pacific and the negative Indian Ocean Dipole (IOD) mode are associated with exceeding rainfall over MIC (Fig. 10.d), which is a mark of a extended monsoon (as mentioned in Fig. 4). This association supports the earlier finding that increased SSTs are associated with extended rainfall during the late monsoon, especially in the central Pacific and the Indo-Pacific Warm Pool (Ghosh et al., 2009; Sabeerali et al., 2014). Furthermore, the pattern of connection associates with the impact of global climate models like the El Niño-Southern Oscillation (ENSO), which changes regional SSTs and rainfall distributions in the Indo-Pacific area.

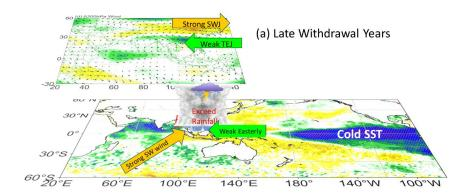
To confirm this SST anomaly influence over regional rainfall or moisture flux patterns, we performed the correlation between 850-hPa moisture transport strength over MIC and Indo-Pacific SST (Fig S-9.e, supplementary). The negative regression coefficients over the central Pacific and the northern western Indian Ocean indicate that negative ENSO and IOD enhance moisture transport at lower levels (Fig. 10.e). The correlation and regression results all together point to the critical role of SSTs in driving the extended moisture convergence that maintains convective activity and delays monsoon withdrawal (Roxy et al., 2019; Sharmila et al., 2013).

In addition, the correlation matrix in Fig. 10.f summarizes the links among the main variables of the research, including the MSwM withdrawal index, TEJ, SWJ, rainfall (RF), 850-hPa moisture transport, and indices indicative of ENSO and IOD. This exhibited the anomalous SSTs, especially in the central Pacific and northern Indian Ocean, significantly influence the intensity of the TEJ and SWJ, as well as moisture transport and rainfall patterns. The weakened TEJ, strengthened SWJ, and positive moisture convergence led to the well-known delay of MSwM departure (Fig. 11). The results align with the current literature connecting SST anomalies, major climate models like ENSO and IOD, and monsoon variability (Ding et al., 2011b; Jia et al., 2013; Krishnamurthy & Kirtman, 2009).





Comprehending these linkages enhances long-term predictions and prepares agricultural systems for modifications in the southwest monsoon departure date from MIC.



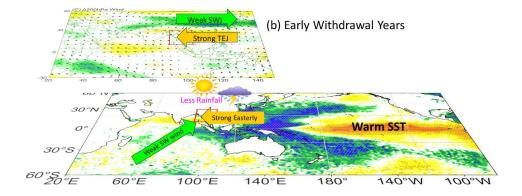


Fig. 11 Air-Sea interaction Dynamical schematic of (a) late and (b) early withdrawal years. This figure was created with Python 3.10 (Matplotlib 3.5.2 [https://matplotlib.org/], Cartopy 0.20.0 [https://pypi.org/project/Cartopy/]).

4 Conclusion

 Focusing on the timing of the monsoon onset and withdrawal, the study offers vital insights into the changing dynamics and interannual variability of the Mainland Indochina Southwest Monsoon (MSwM). With the development of the Cumulative Change of the MSwM (CPM) index, a more thorough knowledge of monsoon transitions may be achieved than with typical daily measurements. This index effectively captures the continuous build-up of crucial atmospheric components.

Withdrawal timing has been noticeably delayed over the past few decades, according to the findings, which also show clear patterns in the start and withdrawal phases. SWJ and the TEJ, which control the monsoon withdrawal processes, have had a significant impact on this delay. Additionally, the MSwM atmospheric circulation and moisture transport are significantly influenced by SST

https://doi.org/10.5194/egusphere-2025-1159 Preprint. Discussion started: 16 April 2025 © Author(s) 2025. CC BY 4.0 License.





anomalies, especially in the western Pacific and Indian Oceans. In mainland Indochina, extended monsoon seasons increase the risk of flooding and interfere with agricultural cycles, underscoring the urgent need for efficient water management and flexible farming techniques.

As conclusion, the MSwM CPM index is a great tool for tracking monsoon variability, and the framework it gives for studying how climate change is affecting the regional monsoon system through composite correlation and trend analysis is invaluable. Improving our understanding of monsoon behavior and constructing more accurate prediction models will require further studies, specifically on the teleconnection mechanisms between large-scale climatic drivers (such ENSO and IOD) and MSwM.





- 480 Data Availability
- 481 Source Data
- 482 All Reanalysis rainfall, wind components, OLR, and Mean Seal Level Pressure netcdf4 data for this
- study were downloaded from the NCEP and ECMWF data portal.
- 484 The historical record of onset and withdrawal dates by DMH of Myanmar the actual monthly rainfall
- 485 observation data and mean sea level pressure data from 79 observation stations used to support the
- 486 findings of this study was provided under permission by Myanmar's Department of Meteorology and
- 487 Hydrology (DMH) and hence cannot be freely distributed. Requests for access to these data should be
- made to the Director-General of DMH, Myanmar. https://www.moezala.gov.mm/
- 489 Software availability
- 490 Open Grads (http://opengrads.org/), Climate data operator (https://code.mpimet.mpg.de/), Python and
- 491 IBM SPSS are mainly used for this study. Among these first two are open-source applications for
- 492 everyone. Codes are also available upon request.

493 Conflicts of Interest

- 494 I declared that there is no potential conflict of interest with any of the following statements.
- 1. For any component of the submitted work, the author received no cash or services from a third party (government, commercial, private foundation, etc). (including but not limited to grants, data monitoring board, study design, manuscript preparation, statistical analysis, etc.).
- 498 2. The author is not affiliated with any entity that has a direct or indirect financial interest in the manuscript's subject matter.
- 3. The author was involved in the following aspects of the project: (a) idea and design, or data analysis and interpretation; (b) authoring the article or critically reviewing it for essential intellectual content; and (c) approval of the final version.
- 503 4. This work has not been submitted to, and is not currently being reviewed by, any other journal or publishing venue.
- 505 5. The author has no patents that are broadly relevant to the work, whether proposed, pending, or issued.
- 507 6. The author received no payment or services from a third party for any aspect of the submitted work (government, commercial, private foundation, etc). (including but not limited to grants, data monitoring board, study design, manuscript preparation, statistical analysis, etc.).

Funding Statement

510

511 This study is supported by the National Natural Science Foundation of China (Grant 42088101).



513

514

515

516

517

518

519

520

521

522



Acknowledgment

The researcher expresses special thanks to all Professors who approve and support this research and Nanjing University of Information Science for support to come out of this research. I would also like to extend my gratitude to Professor Haishan Chen from Nanjing University of Information Science and Technology, for supervisor this paper and his others, support during this research. The author acknowledges heartfelt thanks to the scientists of the ECMFW for supporting ERA5 datasets and the Department of Meteorology and Hydrology for support the data of Myanmar. Additionally, the author would like to thank three reviewers for their constructive and insightful reviews and comments which have significantly helped to improve the manuscript. First author Kyaw Than Oo would like to show his gratitude to Mrs Moh Moh Zaw Thin from UIBE, China for her physical and mental support for this work.

523 **Author Contribution**

- 524 **Kyaw Than Oo:** Conceptualization, methodology, data curation, writing- original draft preparation.,
- 525 visualization and investigation.
- 526 **Haishan Chen**: Supervision.
- 527 **Kazora Jonah**: Writing review & editing.
- 528 **Xinguan Du**: Writing review & editing.

529530

531

536

537

538

539

540

References

- Ajayamohan, R. S., Rao, S. A., Luo, J. J., & Yamagata, T. (2009). Influence of Indian Ocean
 Dipole on boreal summer intraseasonal oscillations in a coupled general circulation model.
 Journal of Geophysical Research Atmospheres, 114(6).
 https://doi.org/10.1029/2008JD011096
 - Akter, N., & Tsuboki, K. (2014). Role of synoptic-scale forcing in cyclogenesis over the Bay of Bengal. *Climate Dynamics*, 43(9–10), 2651–2662. https://doi.org/10.1007/S00382-014-2077-9/METRICS
 - 3. Aung, L. L., Zin, E. E., Theingi, P., Elvera, N., Aung, P. P., Han, T. T., Oo, Y., & Skaland, R. G. (2017). Myanmar Climate Report. *Norwgian Meterological Institute*, *9*, 105.
- Bombardi, R. J., Kinter, J. L., & Frauenfeld, O. W. (2019). A global gridded dataset of the characteristics of the rainy and dry seasons. *Bulletin of the American Meteorological Society*, 100(7), 1315–1328. https://doi.org/10.1175/BAMS-D-18-0177.1
- 5. Bordoni, S., & Schneider, T. (2008). Monsoons as eddy-mediated regime transitions of the tropical overturning circulation. *Nature Geoscience*, 1(8), 515–519. https://doi.org/10.1038/NGEO248
- 547 6. Breiman, L. (2001). Random forests. *Machine Learning*, 45(1), 5–32. 548 https://doi.org/10.1023/A:1010933404324





- Cao, J., Hu, J., & Tao, Y. (2012). An index for the interface between the Indian summer monsoon and the East Asian summer monsoon. *Journal of Geophysical Research Atmospheres*,
 117(17), 1–9. https://doi.org/10.1029/2012JD017841
- 552 8. Chen, L., Chen, W., Hu, P., Chen, S., & An, X. (2023). Climatological characteristics of the East Asian summer monsoon retreat based on observational analysis. *Climate Dynamics*, 60(9–10), 3023–3037. https://doi.org/10.1007/s00382-022-06489-6
- Chen, M., Shi, W., Xie, P., Silva, V. B. S., Kousky, V. E., Higgins, R. W., & Janowiak, J. E.
 (2008). Assessing objective techniques for gauge-based analyses of global daily precipitation.
 Journal of Geophysical Research Atmospheres, 113(4).
 https://doi.org/10.1029/2007JD009132
- 559 10. Chou, C., Neelin, J. D., Chen, C. A., & Tu, J. Y. (2009). Evaluating the "rich-get-richer" 560 mechanism in tropical precipitation change under global warming. *Journal of Climate*, 22(8), 1982–2005. https://doi.org/10.1175/2008JCLI2471.1
- 562 11. Colbert, A. J., Soden, B. J., & Kirtman, B. P. (2015). The impact of natural and anthropogenic 563 climate change on western North Pacific tropical cyclone tracks. *Journal of Climate*, 28(5), 564 1806–1823. https://doi.org/10.1175/JCLI-D-14-00100.1
- 565 12. CY Li, L. Z. (1999). Activity of the South China Sea summer monsoon and it effect. *Acta Atmos Sinica*, 23, 257–266.
- 13. Dimri, A. P., Niyogi, D., Barros, A. P., Ridley, J., Mohanty, U. C., Yasunari, T., & Sikka, D.
 R. (2015). Reviews of Geophysics Western Disturbances: A review. *Reviews of Geophysics*,
 53, 225–246. https://doi.org/10.1002/2014RG000460.Received
- 570 14. Ding, Q., Wang, B., Wallace, J. M., & Branstator, G. (2011a). Tropical-extratropical teleconnections in boreal summer: Observed interannual variability. *Journal of Climate*, 24(7), 1878–1896. https://doi.org/10.1175/2011JCLI3621.1
- 573 15. Ding, Q., Wang, B., Wallace, J. M., & Branstator, G. (2011b). Tropical-extratropical teleconnections in boreal summer: Observed interannual variability. *Journal of Climate*, 24(7), 1878–1896. https://doi.org/10.1175/2011JCLI3621.1
- 576 16. Evan, A. T., & Camargo, S. J. (2011). A climatology of Arabian Sea cyclonic storms. *J Clim*, 577 24(1), 140–158. https://doi.org/10.1175/2010jcli3611.1
- 578 17. Fasullo, J., & Webster, P. J. (2003). A hydrological definition of Indian Monsoon onset and withdrawal. *Journal of Climate*, *16*(19), 3200–3211. https://doi.org/10.1175/1520-0442(2003)016<3200a:AHDOIM>2.0.CO;2
- 581 18. Fosu, B. O., & Wang, S. Y. S. (2015). Bay of Bengal: coupling of pre-monsoon tropical cyclones with the monsoon onset in Myanmar. *Climate Dynamics*, 45(3–4), 697–709. https://doi.org/10.1007/s00382-014-2289-z
- 584 19. Ghosh, S., Luniya, V., & Gupta, A. (2009). Trend analysis of Indian summer monsoon rainfall 585 at different spatial scales. *Atmospheric Science Letters*, 10(4), 285–290. 586 https://doi.org/10.1002/ASL.235
- 587 20. Goswami, B. N., Krishnamurthy, V., & Annmalai, H. (1999). A broad-scale circulation index 588 for the interannual variability of the Indian summer monsoon. *Quarterly Journal of the Royal* 589 *Meteorological Society*, 125(554), 611–633. https://doi.org/10.1002/qj.49712555412
- 590 21. Goswami, B. N., & Xavier, P. K. (2005). ENSO control on the south Asian monsoon through 591 the length of the rainy season. *Geophys Res Lett*, 32(18), L18717. 592 https://doi.org/10.1029/2005g1023216
- 593 22. Hannachi, A. (2004). A primer for EOF analysis of climate data. Reading: University of



596

597

598

599

603

604



- Reading, 1–33. http://www.o3d.org/eas-6490/lectures/EOFs/eofprimer.pdf
 - 23. Hersbach, H., Bell, B., Berrisford, P., Hirahara, S., Horányi, A., Muñoz-Sabater, J., Nicolas, J., Peubey, C., Radu, R., Schepers, D., Simmons, A., Soci, C., Abdalla, S., Abellan, X., Balsamo, G., Bechtold, P., Biavati, G., Bidlot, J., Bonavita, M., ... Thépaut, J. N. (2020). The ERA5 global reanalysis. *Quarterly Journal of the Royal Meteorological Society*, *146*(730), 1999–2049. https://doi.org/10.1002/QJ.3803
- 600 24. Htway, O., & Matsumoto, J. (2011). Climatological onset dates of summer monsoon over 601 Myanmar. *International Journal of Climatology*, 31(3), 382–393. 602 https://doi.org/10.1002/JOC.2076
 - 25. Hu, P., Chen, W., Chen, S., & Huang, R. (2019). Interannual variability and triggers of the South China Sea summer monsoon withdrawal. *Climate Dynamics*, 53(7–8), 4355–4372. https://doi.org/10.1007/s00382-019-04790-5
- 26. Hu, P., Chen, W., Wang, L., Chen, S., Liu, Y., & Chen, L. (2022). Revisiting the ENSO-monsoonal rainfall relationship: new insights based on an objective determination of the Asian summer monsoon duration. *Environmental Research Letters*, 17(10). https://doi.org/10.1088/1748-9326/ac97ad
- 610 27. Huang, S., Wang, B., & Wen, Z. (2020). Dramatic weakening of the tropical easterly jet 611 projected by CMIP6 models. *Journal of Climate*, 33(19), 8439–8455. 612 https://doi.org/10.1175/JCLI-D-19-1002.1
- 28. Jia, X., Yang, S., Li, X., Liu, Y., Wang, H., Liu, X., & Weaver, S. (2013). Prediction of global patterns of dominant quasi-biweekly oscillation by the NCEP Climate Forecast System version 2. *Climate Dynamics*, 41(5–6), 1635–1650. https://doi.org/10.1007/S00382-013-1877-7
- 29. Jiao, D., Xu, N., Yang, F., & Xu, K. (2021). Evaluation of spatial-temporal variation performance of ERA5 precipitation data in China. *Scientific Reports*, 11(1), 1–13. https://doi.org/10.1038/s41598-021-97432-y
- 619 30. K Lau, K. K. S. Y. (2000). Dynamical and boundary forcing characteristics of regional components of the Asian summer monsoon. *J Clim*, 13, 2461–2482. https://doi.org/10.1175/1520-0442(2000)013<2461:dabfco>2.0.co
- 31. Kanamitsu, M., Ebisuzaki, W., Woollen, J., Yang, S. K., Hnilo, J. J., Fiorino, M., & Potter, G.
 L. (2002). NCEP-DOE AMIP-II reanalysis (R-2). Bulletin of the American Meteorological
 Society, 83(11). https://doi.org/10.1175/BAMS-83-11-1631
- 32. Kotal, S. D., Bhattacharya, S. K., Roy Bhowmik, S. K., & Kundu, P. K. (2014). Growth of
 cyclone Viyaru and Phailin—A comparative study. *J. Earth Syst. Sci.*, 123(7), 1619–1635.
 https://doi.org/10.1007/s12040-014-0493-1
- 33. Krishnamurthy, V., & Kirtman, B. P. (2009). Relation between Indian monsoon variability and SST. *Journal of Climate*, 22(17), 4437–4458. https://doi.org/10.1175/2009JCLI2520.1
- 34. Krugman, P. R., Obstfeld, M., & Melitz, M. J. T. A.-T. T.-. (2018). International economics:
 theory & policy (Eleventh e). Pearson New York. https://doi.org/LK https://worldcat.org/title/1014329502
- 35. Li, H., Dai, A., Zhou, T., & Lu, J. (2010). Responses of East Asian summer monsoon to
 historical SST and atmospheric forcing during 1950-2000. *Climate Dynamics*, 34(4), 501–514.
 https://doi.org/10.1007/S00382-008-0482-7
- 36. Liu, Y., Cook, K. H., & Vizy, E. K. (2021). Delayed retreat of the summer monsoon over the
 Indochina Peninsula linked to surface warming trends. *International Journal of Climatology*,
 41(3), 1927–1938. https://doi.org/10.1002/JOC.6938



653

654

661

662



- 37. Loikith, P. C., Pampuch, L. A., Slinskey, E., Detzer, J., Mechoso, C. R., & Barkhordarian, A.
 (2019). A climatology of daily synoptic circulation patterns and associated surface
 meteorology over southern South America. *Climate Dynamics*, 53(7–8), 4019–4035.
 https://doi.org/10.1007/S00382-019-04768-3/FIGURES/12
- 38. Ma, Y. Z. (2019). Quantitative Geosciences: Data Analytics, Geostatistics, Reservoir Characterization and Modeling. In *Quantitative Geosciences: Data Analytics, Geostatistics, Reservoir Characterization and Modeling*. https://doi.org/10.1007/978-3-030-17860-4
- 39. Mao, J., & Wu, G. (2007). Interannual variability in the onset of the summer monsoon over the
 Eastern Bay of Bengal. *Theoretical and Applied Climatology*, 89(3–4), 155–170.
 https://doi.org/10.1007/S00704-006-0265-1
- 649 40. Oo, K. T. (2022a). Interannual Variability of Winter Rainfall in Upper Myanmar. *Journal of Sustainability and Environmental Management*, 1(3), 344–358. https://doi.org/10.3126/josem.v1i3.48001
 - 41. Oo, K. T. (2022b). Interannual Variability of Winter Rainfall in Upper Myanmar. *Journal of Sustainability and Environmental Management*, 1(3), 344–358. https://doi.org/https://doi.org/10.3126/josem.v1i3.48001
- 42. Oo, K. T. (2023a). Climatology Definition of the Myanmar Southwest Monsoon (MSwM):
 Change Point Index (CPI). Advances in Meteorology, 2023, 2346975.
 https://doi.org/10.1155/2023/2346975
- 43. Oo, K. T. (2023b). Climatology Definition of the Myanmar Southwest Monsoon (MSwM):
 Change Point Index (CPI). Advances in Meteorology, 2023, 2346975.
 https://doi.org/10.1155/2023/2346975
 - 44. Oo, K. T., Chen, H., Dong, Y., & Jonah, K. (2024). Investigating the link between Mainland-Indochina monsoon onset dates and cyclones over the Bay of Bengal basin. *Climate Dynamics*. https://doi.org/10.1007/S00382-024-07342-8
- 45. Oo, K. T., & Jonah, K. (2024). Interannual variation of summer southwest monsoon rainfall
 over the monsoon core regions of the eastern Bay of Bengal and its relationship with oceans.
 Journal of Atmospheric and Solar-Terrestrial Physics, 265, 106341.
 https://doi.org/10.1016/J.JASTP.2024.106341
- 46. Q Guo, J. W. (1988). A comparison of the summer precipitation in India with that in China. *J Trop Meteorol*, 4, 53–60.
- 47. Ramage, C. S. (1971). *Monsoon meteorology*. Academic Press.
- 48. Ren, Q., Liu, F., Wang, B., Yang, S., Wang, H., & Dong, W. (2022). Origins of the
 Intraseasonal Variability of East Asian Summer Precipitation. *Geophysical Research Letters*,
 49(4). https://doi.org/10.1029/2021GL096574
- 49. Roxy, M. K., Dasgupta, P., McPhaden, M. J., Suematsu, T., Zhang, C., & Kim, D. (2019).
 Twofold expansion of the Indo-Pacific warm pool warps the MJO life cycle. *Nature*, 575(7784),
 647–651. https://doi.org/10.1038/s41586-019-1764-4
- 50. Roxy, M. K., Ritika, K., Terray, P., & Masson, S. (2014). The curious case of Indian Ocean warming. *Journal of Climate*, 27(22), 8501–8509. https://doi.org/10.1175/JCLI-D-14-00471.1
- 51. Sabeerali, C. T., Rao, S. A., George, G., Nagarjuna Rao, D., Mahapatra, S., Kulkarni, A., & Murtugudde, R. (2014). Modulation of monsoon intraseasonal oscillations in the recent warming period. *Journal of Geophysical Research*, 119(9), 5185–5203. https://doi.org/10.1002/2013JD021261
- 683 52. Salinger, M. J., Shrestha, M. L., Ailikun, Dong, W., McGregor, J. L., & Wang, S. (2014).



691

692

700

701

702



- Climate in Asia and the Pacific: Climate Variability and Change. *Advances in Global Change Research*, *56*, 17–57. https://doi.org/10.1007/978-94-007-7338-7_2
- 53. Sawyer, J. S. (1947). The structure of the intertropical front over N.W. India during the S.W.
 Monsoon. *Quarterly Journal of the Royal Meteorological Society*, 73(317–318), 346–369.
 https://doi.org/10.1002/QJ.49707331709
- 54. Schmidhammer. (2000). Box Plot and Robust Statistics. *Matrix*, 5, 109–122.
 - 55. Seager, R., Naik, N., & Vecchi, G. A. (2010). Thermodynamic and dynamic mechanisms for large-scale changes in the hydrological cycle in response to global warming. *Journal of Climate*, 23(17), 4651–4668. https://doi.org/10.1175/2010JCLI3655.1
- 56. Selman, C., & Misra, V. (2014). The Met Office Hadley Centre sea ice and sea surface
 temperature data set, version 2: 1. Sea ice concentrations. *Journal of Geophysical Research*, 3,
 180–198. https://doi.org/10.1002/2013JD021040.Received
- 57. Sharmila, S., Pillai, P. A., Joseph, S., Roxy, M., Krishna, R. P. M., Chattopadhyay, R., Abhilash,
 S., Sahai, A. K., & Goswami, B. N. (2013). Role of ocean-atmosphere interaction on northward
 propagation of Indian summer monsoon intra-seasonal oscillations (MISO). *Climate Dynamics*,
 41(5–6), 1651–1669. https://doi.org/10.1007/S00382-013-1854-1
 - 58. Sreekala, P. P., Bhaskara Rao, S. V., Arunachalam, M. S., & Harikiran, C. (2014). A study on the decreasing trend in tropical easterly jet stream (TEJ) and its impact on Indian summer monsoon rainfall. *Theoretical and Applied Climatology*, 118(1–2), 107–114. https://doi.org/10.1007/s00704-013-1049-z
- 59. Vijaya Kumari, K., Karuna Sagar, S., Viswanadhapalli, Y., Dasari, H. P., & Bhaskara Rao, S.
 V. (2018). Role of planetary boundary layer processes on the simulation of tropical cyclones over Bay of Bengal. *Pure and Applied Geophysics*, 176(2), 951–977.
 https://doi.org/10.1007/s00024-018-2017-4
- 60. Walker, J. M., Bordoni, S., & Schneider, T. (2015). Interannual variability in the large-scale
 dynamics of the South Asian summer monsoon. *Journal of Climate*, 28(9), 3731–3750.
 https://doi.org/10.1175/JCLI-D-14-00612.1
- 711 61. Wang, B., & Ho, L. (2002). Rainy season of the Asian-Pacific summer monsson. *Journal of Climate*, 15(4), 386–398. https://doi.org/10.1175/1520-0442(2002)015<0386:RSOTAP>2.0.CO:2
- 714 62. Wang, B., LinHo, Zhang, Y., & Lu, M. M. (2004). Definition of South China Sea monsoon onset and commencement of the East Asian summer monsoon. *Journal of Climate*, *17*(4), 699–716 710. https://doi.org/10.1175/2932.1
- 717 63. Wang, B., Wu, R., & Lau, K. M. (2001). Interannual variability of the asian summer monsoon:
 718 Contrasts between the Indian and the Western North Pacific-East Asian monsoons. *Journal of Climate*, 14(20), 4073–4090. https://doi.org/10.1175/1520-720 0442(2001)014<4073:IVOTAS>2.0.CO;2
- 64. Wang, B., Wu, Z., Li, J., Liu, J., Chang, C. P., Ding, Y., & Wu, G. (2008). How to measure the
 strenght of the East Asian summer monsoon. *Journal of Climate*, 21(17), 4449–4463.
 https://doi.org/10.1175/2008JCLI2183.1
- 724 65. Webster, P. J., & Yang, S. (1992). Monsoon and Enso: Selectively Interactive Systems. 725 *Quarterly Journal of the Royal Meteorological Society*, 118(507), 877–926. 726 https://doi.org/10.1002/qj.49711850705
- 727 66. Win Zin, W., & Rutten, M. (2017). Long-term Changes in Annual Precipitation and Monsoon 728 Seasonal Characteristics in Myanmar. *Hydrology: Current Research*, 08(02).

https://doi.org/10.5194/egusphere-2025-1159 Preprint. Discussion started: 16 April 2025 © Author(s) 2025. CC BY 4.0 License.





- 729 https://doi.org/10.4172/2157-7587.1000271
- 730 67. Wu, R. (2017). Relationship between Indian and East Asian summer rainfall variations. 731 *Advances in Atmospheric Sciences*, 34(1), 4–15. https://doi.org/10.1007/S00376-016-6216-6
- 68. Wu, X., & Mao, J. (2018). Spatial and interannual variations of spring rainfall over eastern China in association with PDO–ENSO events. *Theoretical and Applied Climatology*, *134*(3–4), 935–953. https://doi.org/10.1007/s00704-017-2323-2
- 735 69. Xu, C., Wang, S. Y. S., Borhara, K., Buckley, B., Tan, N., Zhao, Y., An, W., Sano, M., Nakatsuka, T., & Guo, Z. (2023). Asian-Australian summer monsoons linkage to ENSO strengthened by global warming. *Npj Climate and Atmospheric Science*, *6*(1). https://doi.org/10.1038/S41612-023-00341-2
- 70. Zhang, S., Qu, X., Huang, G., Hu, P., Zhou, S., & Wu, L. (2024). Delayed Onset of Indian Summer Monsoon in Response to CO2 Removal. *Earth's Future*, *12*(2), 1–17. https://doi.org/10.1029/2023EF004039
- 71. Zhang, Y., Li, T., Wang, B., & Wu, G. (2002a). Onset of the summer monsoon over the Indochina Peninsula: Climatology and interannual variations. *Journal of Climate*, *15*(22), 3206–3221. https://doi.org/10.1175/1520-0442(2002)015<3206:OOTSMO>2.0.CO;2
- 72. Zhang, Y., Li, T., Wang, B., & Wu, G. (2002b). Onset of the Summer Monsoon over the Indochina Peninsula: Climatology and Interannual Variations. *Journal of Climate*, 15(22), 3206–3221.https://doi.org/https://doi.org/10.1175/1520-0442(2002)015<3206:OOTSMO>2.0.CO;2
 - 73. Zin Mie Mie Sein, B. Ogwang, V. Ongoma, Faustin Katchele Ogou, & Kpaikpai Batebana. (2015). *Inter-annual variability of Summer Monsoon Rainfall over Myanmar in relation to IOD and ENSO* (pp. 4:28-36). Journal of Environmental and Agricultural Sciences.

751752

749